RNase T1 Variant RV Cleaves Single-Stranded RNA after Purines Due to Specific Recognition by the Asn46 Side Chain Amide

Rico Czaja,[‡] Marc Struhalla,[‡] Katja Höschler,[‡] Wolfram Saenger,[§] Norbert Sträter,[||] and Ulrich Hahn*[,‡]

Department of Chemistry, Division of Biochemistry and Molecular Biology, Hamburg University, Martin-Luther-King-Platz 6, 20146 Hamburg, Germany, Institute of Crystallography, Free University of Berlin, Takusstrasse 6, 14195 Berlin, Germany, and Biotechnological and Biomedical Centre, University of Leipzig, Am Deutschen Platz 5, 04103 Leipzig, Germany

Received November 4, 2003; Revised Manuscript Received January 15, 2004

ABSTRACT: Attempts to alter the guanine specificity of ribonuclease T1 (RNase T1) by rational or random mutagenesis have failed so far. The RNase T1 variant RV (Lys41Glu, Tyr42Phe, Asn43Arg, Tyr45Trp, and Glu46Asn) designed by combination of a random and a rational mutagenesis approach, however, exhibits a stronger preference toward adenosine residues than wild-type RNase T1. Steady state kinetics of the cleavage reaction of the two dinucleoside phosphate substrates adenylyl-3′,5′-cytidine and guanylyl-3′,5′-cytidine revealed that the ApC/GpC ratio of the specificity coefficient (k_{cat}/K_m) was increased ∼7250-fold compared to that of the wild-type. The crystal structure of the nucleotide-free RV variant has been refined in space group $P6_1$ to a crystallographic *R*-factor of 19.9% at 1.7 Å resolution. The primary recognition site of the RV variant adopts a similar conformation as already known from crystal structures of RNase T1 not complexed to any nucleotide. Noteworthy is a high flexibility of Trp45 and Asn46 within the three individual molecules in the asymmetric unit. In addition to the kinetic studies, these data indicate the participation of Asn46 in the specific recognition of the base and therefore a specific binding of adenosine.

Ribonuclease T1 (RNase T1, EC 3.1.27.3) represents an ideal model system for studying structure−function relationships of protein enzymes. RNase T1 is a small globular, well-characterized enzyme from the mold fungus *Aspergillus oryzae*. It is the key member of the so-called RNase T1 family, a group of microbial RNases of fungal and bacterial origin (*1*, *2*). The enzyme consists of 104 amino acid residues with a relative molecular mass of 11 089 Da. It cleaves single-stranded RNA with high specificity at guanylyl residues, yielding new guanosine 3′-phosphates and 5′-OH in a two-step mechanism with guanosine 2′,3′-cyclic phosphate as the intermediate (*3*, *4*).

The crystal structures of the enzyme complexed with the inhibitor 2′-GMP (*5*, *6*), with the cleavage product 3′-GMP (*7*, *8*), with the dinucleoside phosphate inhibitor 2′,5′-GpG (*9*), with 2′-AMP (*10*), and with an unoccupied recognition site (*11*, *12*) have each been determined at high resolution. These data revealed that the specific recognition of the guanine base by the enzyme is due to interactions between the nucleobase and a protein loop consisting of residues 42−46 together with residue 98. The guanine base is involved in extensive hydrogen bonding with main chain atoms (Asn43 NH···Gua N7, Asn44 NH···Gua O6, and Tyr45 NH···Gua O6), and the GuaN2H forms a hydrogen bond to the peptidic oxygen of Asn98 which is located outside the recognition loop. The only amino acid that interacts with its side chain with the base is the glutamate in position 46, forming Gua N1H···Glu46 Oϵ1 and Gua N2H···Glu46 Oϵ2 bidentate hydrogen bonds (Figure 1a). In addition, the side chains of Tyr42 and Tyr45 form a hydrophobic pocket and sandwich the guanine base, whereby it is thought that Tyr45 acts as a lid covering the base. Within the RNase T1 family, Glu46 is highly conserved. Attempts to design RNase T1 variants with altered specificity were based on the mentioned crystal structures or sequence alignments. Starting points for rational mutagenesis studies were tyrosines 42 and 45 which were involved in guanine recognition by sandwiching the guanine with their side chains as well as Glu46 (*13*−*18*). All of these mutations did not alter nucleotide specificity. Substitutions of Tyr42 and Tyr45 led to variants with both increased (*14*, *17*) and decreased (*14*, *16*) catalytic activity. Substitutions of Glu46 also led to variants with extremely decreased catalytic activity (*13*, *16*), although it was suggested that the Glu46Ala and Glu46Gln variants (due to specific possible bidentate hydrogen bond formation with the Gln46 amide and adenine) would have greater relative affinities for adenine than the wild-type as shown in Figure 1b for the Glu46Gln variant (*19*). The crystal structures of the Glu46Gln variant in complex with both 2′-GMP and 2′-AMP showed that both nucleotides do not bind the enzyme in the guanine recognition site but at the 3′-subsite at His92 (*13*). The side chain of Gln46 is tightly hydrogen bonded to main chains atoms of Phe100 and locks the guanine binding site, and therefore, this variation does not lead to a change in the RNase T1 specificity but to a significant loss of catalytic activity. Random mutagenesis studies of the complete primary recognition site (*20*) did also not lead to variants with altered specificity. The complete randomization

* To whom correspondence should be addressed. Phone: +49 (0) 40-42838 3214. Fax: +49 (0) 40-42838 2848. E-mail: uli.hahn@uni-hamburg.de.

[‡] Hamburg University.

[§] Free University of Berlin.

[||] University of Leipzig.

10.1021/bi035961f CCC: $27.50 © 2004 American Chemical Society
Published on Web 02/20/2004

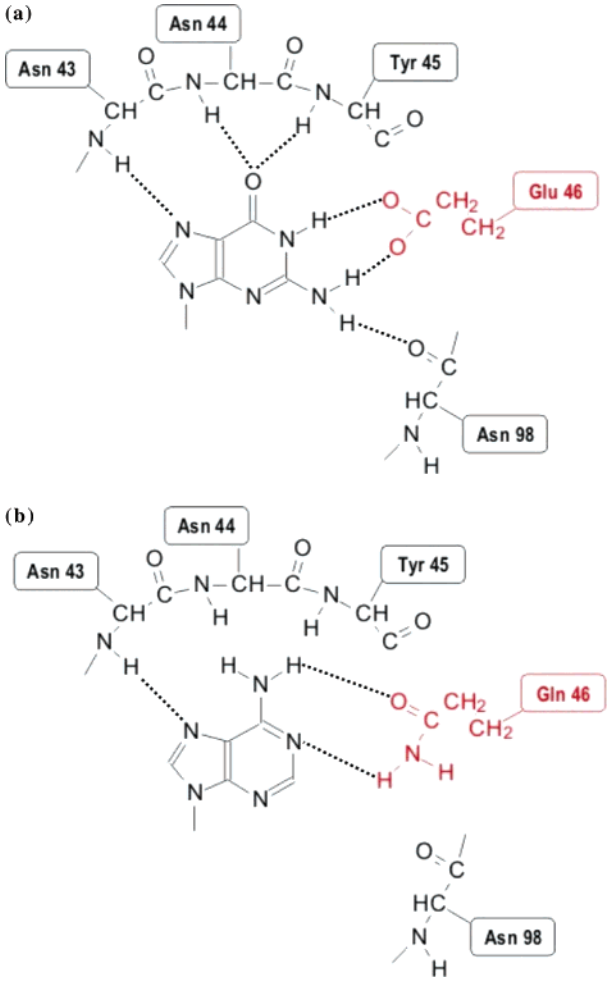

FIGURE 1: Schematic representation of the primary recognition site of (a) RNase T1-wt with a bound guanine base and (b) hypothetical binding of an adenine base to RNase T1 variant E46Q predicted on the basis of theoretical molecular dynamics and free energy perturbation calculations (*19*). The protein backbone of amino acids 43−45 and 98 and the side chains of Glu46 and Gln46 are shown. Hydrogen bonds are represented with dashed lines.

of this recognition site yielded a combinatorial library of 1.6 million variants. One hundred eighty of these variants exhibited RNA cleaving activity, however, without any change in substrate specificity. Comparisons of the primary structures revealed a conservation of the amino acid in position 46 that was mainly occupied by glutamate or the similar residue aspartate. Only in one active variant was the glutamate substituted with glutamine, a substitution leading to inactivation via a single-point mutation (*13*). The primary recognition site of this so-called 9/5 variant is completely different from that of the wild-type (wt)[1] and exhibited the 41-GluPheArgAsnTrpGln-46 amino acid sequence instead of the 41-LysTyrAsnAsnTyrGlu-46 amino acid sequence. The crystal structure of this enzyme cocrystallized with 2′-GMP (*21*) shows that the guanine is bound in a different manner to the recognition site in comparison to the Glu46Gln variant, although the glutamine in position 46 does not participate in guanine recognition because it remains tightly hydrogen bonded to Phe100 like in the Glu46Gln variant. The binding of the guanine base is presumably based on the increased level of aromatic stacking due to the Tyr45Trp exchange. But as the glutamine does not take part in substrate recognition in variant 9/5 no change in substrate specificity took place. On the basis of these data, it was suggested that the substitution of Gln46 with Asn in variant 9/5 would lead to a variant that could also recognize adenine. Because of the shortening of this amino acid side chain due to one missing methylene group, the two hydrogen bonds to Phe100 would presumably be impossible to form, whereby the amide group of asparagine would be able to recognize adenosine as it is shown for glutamine in Figure 1b. In this work, we report on the RNase T1 RV with the 41-GluPheArgAsnTrpAsn-46 primary recognition site. This variant was created by genetic engineering, and its biochemical characterization indeed resulted in a significantly altered substrate specificity. Here we report also the crystallographic characterization that led to insights into the adenine recognition of RNase T1 RV.

[1] Abbreviations: wt, wild-type; A*n*, amino acid in position *n* of molecule A in the asymmetric unit.

MATERIALS AND METHODS

Guanylyl-3′,5′-cytidine (GpC) and adenylyl-3′,5′-cytidine (ApC) were from Pharma-Waldhof (Düsseldorf, Germany). Mutagenesis and standard primers were from MWG-Biotech (Ebersberg, Germany). All other chemicals were from Merck (Darmstadt, Germany) and Sigma (Deisenhofen, Germany).

Site-Directed Mutagenesis and Enzyme Purification

RNase T1 RV was constructed by site-directed mutagenesis using two-step PCR (*22*). The mutagenesis primer was 5′-CAC AGA GAA ATC AAA ACC GTT CCA GTT GCG GAA TTC GTG TGG GTA AGA ATT GG-3′ (base substitutions underlined). Standard primers were A2VO (5′-TAC GGA TTC ACT GGA ACT CTA GA-3′) and A2HI (5′-CAT CTT AGC AGC CTG AAC-3′). RNase T1-wt and variant RV were overproduced in *Escherichia coli* XL1 blue harboring the pA2T1 plasmid (*23*). The enzymes were isolated from the periplasm by osmotic shock and purified by DEAE anion exchange and size exclusion chromatography (*24*) to homogeneity. Purity and authenticity were judged by SDS−PAGE and MALDI-MS.

Determination of Substrate Specificity

The substrate specificity was tested by cleavage of GpC and ApC. The enzyme (5 μM) was incubated with GpC or ApC (1 mg/mL, corresponding to 1.65 and 1.75 mM, respectively) in Tris-HCl buffer (10 mM, pH 7.5) containing 1 mM EDTA for 15 min at room temperature. Cleavage products were analyzed by thin-layer chromatography (*3*).

Enzyme Kinetics

Dinucleoside Phosphate Cleavage. To determine the kinetic parameters for dinucleoside phosphate cleavage, the hyperchromic effect during transesterification was measured spectrophotometrically. The reaction was carried out in a Hewlett-Packard 8425A spectrophotometer in MES buffer (100 mM, pH 6.0) containing 100 mM NaCl and 2 mM EDTA at 25 °C. The initial velocities were measured in triplicate at 280 nm for GpC transesterification using the difference extinction coefficient $\Delta\epsilon_{280}$ [2200 M^{-1} cm^{-1} (*25*)] and at 268 nm for ApC transesterification using the difference extinction coefficient $\Delta\epsilon_{268}$ [2120 M^{-1} cm^{-1} (*26*)] at substrate concentrations between 20 and 625 μM for GpC hydrolysis

and between 30 and 370 μM for ApC hydrolysis. The enzyme concentrations were 66 nM for GpC hydrolysis and 500 nM for ApC hydrolysis, depending on the activity. The enzyme concentration was determined spectrophotometrically using a calculated ϵ_{280} extinction coefficient of 21 680 M^{-1} cm^{-1} (*27*). The mixtures without enzyme were preincubated for ~3 min to ensure the absence of autohydrolysis, and reactions were started by adding the enzyme. Michaelis−Menten constants were determined by nonlinear regression using the program GraphPad Prism.

RNA Hydrolysis. Hydrolysis of high-molecular mass RNA was assessed by determining the acid soluble oligonucleotides at 260 nm by a modified test from Anfinsen *et al.* (*28*). A total volume of 1 mL containing 3 mg of yeast RNA in 50 mM Tris-HCl buffer (pH 7.5) containing 2 mM EDTA was incubated with the enzyme for 15 min at 37 °C. Nonhydrolyzed RNA was precipitated on ice for 20 min after the addition of 250 μL of ice-cold 2.5% lanthane nitrate in 30% perchloric acid. After centrifugation, the extinction of the diluted supernatant (1:20) was determined at 260 nm. The specific activity of the enzyme was calculated using the following equation: specific activity (units per milligram) = $[E_{260} - E_{260(\text{blank})}] \times 25/(\text{milligram of protein})$. To determine the blank, the enzyme was omitted from the solution.

Crystallization and Data Collection

The crystals used for data collection were obtained by the hanging drop vapor diffusion method (*29*). A droplet was prepared by mixing an equal volume of the protein solution containing 2 mM RNase T1 RV in 10 mM Tris-HCl buffer (pH 8.5) and of the reservoir solution containing 100 mM Tris-HCl buffer (pH 9.0), 200 mM $MgCl_2$, and 20−22% PEG4000. Hexagonal crystals grew at 6 °C within 4 or 5 days to dimensions of ~1.5 mm × 0.15 mm × 0.15 mm. For cryoprotection, the crystals were soaked for approximately 30 min in the reservoir solution containing 20% glycerol and then flash-frozen in liquid nitrogen. During data collection, the crystals were cooled in a nitrogen stream at 100 K. Data were processed using the DENZO/SCALEPACK program (*30*). The crystals belonged to space group $P6_1$ with *a* and *b* values of 56.5 Å and a *c* of 158.7 Å and contained three molecules per asymmetric unit.

Model Building and Refinement

The structure was determined by the molecular replacement method (*31*) using the program AmoRe (*32*) of the CCP4 package (*33*) and RNase T1 9/5 as the search model [Protein Data Bank entry 1CHO (*21*)] excluding the nucleotide and water molecules. The initial model was refined using CNS (version 1.1) (*34*) and manually rebuilt using the interactive graphics model building program O (*35*). The progress of the refinement was monitored by the decrease in R_{free} (*36*) at each stage of model building, energy minimization, and individual isotropic *B*-factor refinement.

RESULTS AND DISCUSSION

Crystal Structure Analysis

The crystals of RNase T1 RV belong to hexagonal space group $P6_1$, and the structure was determined by molecular replacement using T1 variant 9/5 [PDB entry 1CHO (*21*)]. The model was refined to an *R*-factor of 19.9% using X-ray diffraction data to 1.7 Å. The final model consists of 3 × 104 amino acid residues from three individual molecules (named A, B, and C) in the asymmetric unit, 274 water molecules, and two Tris molecules bound to molecules A and C. The entire molecules are well-defined in the electron density map, and only very few side chains at the protein surface appear to be disordered. The ψ and φ torsion angles of all residues are located in the allowed regions of the Ramachandran plot. Alternative conformations were introduced for residues A17, B17, C17, and C28 and for the Arg43−Asn44 peptide bond in molecule A. The data collection and refinement statistics are summarized in Table 1.

Table 1: Parameters for Data Collection and Refinement

data collection	
source	BW7B (DESY)
wavelength (Å)	0.8459
no. of reflections (total/unique)	70573/31400
completeness (%)	90.6
R_{sym} (%)	3.7
Ramachandran parameters	
residues in most favored regions	240 (93%)
residues in additional allowed regions	18 (7%)
residues in generously allowed regions	0 (0%)
refinement	
resolution range (Å)	20−1.7
R-factor (%)	19.9
R_{free} (%)	24.4
rms deviations from ideality	
bond lengths (Å)	0.015
bond angles (deg)	1.74
dihedrals (deg)	24.96
improper dihedrals (deg)	1.11
PDB entry	1Q9E

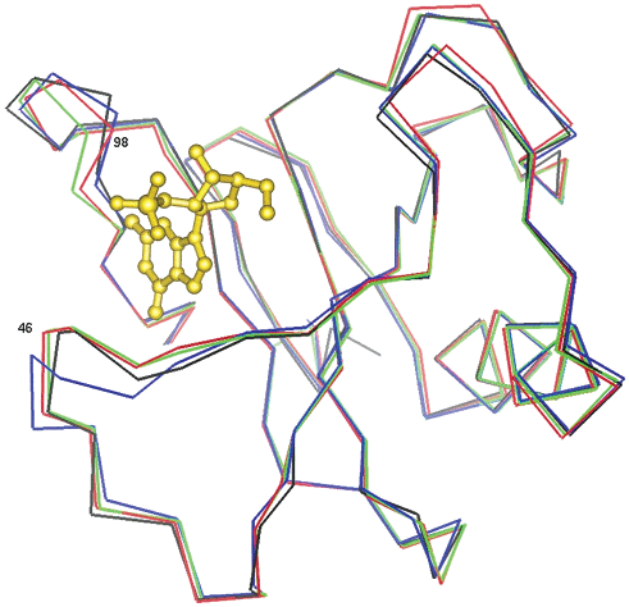

FIGURE 2: Comparison of the three molecules of RNase T1 RV in the asymmetric unit. The protein backbone is shown as a C_α representation (molecule A in red, molecule B in green, and molecule C in blue). Also shown in black is the wt enzyme in complex with 2′-GMP (in gold).

The overall structure of the three molecules of the asymmetric unit is very similar. The rms deviations for the superposition of the C_α atoms of molecules B and C onto molecule A are 0.352 and 0.557 Å, respectively, and 0.582 Å for the superposition of molecule B onto molecule C. The

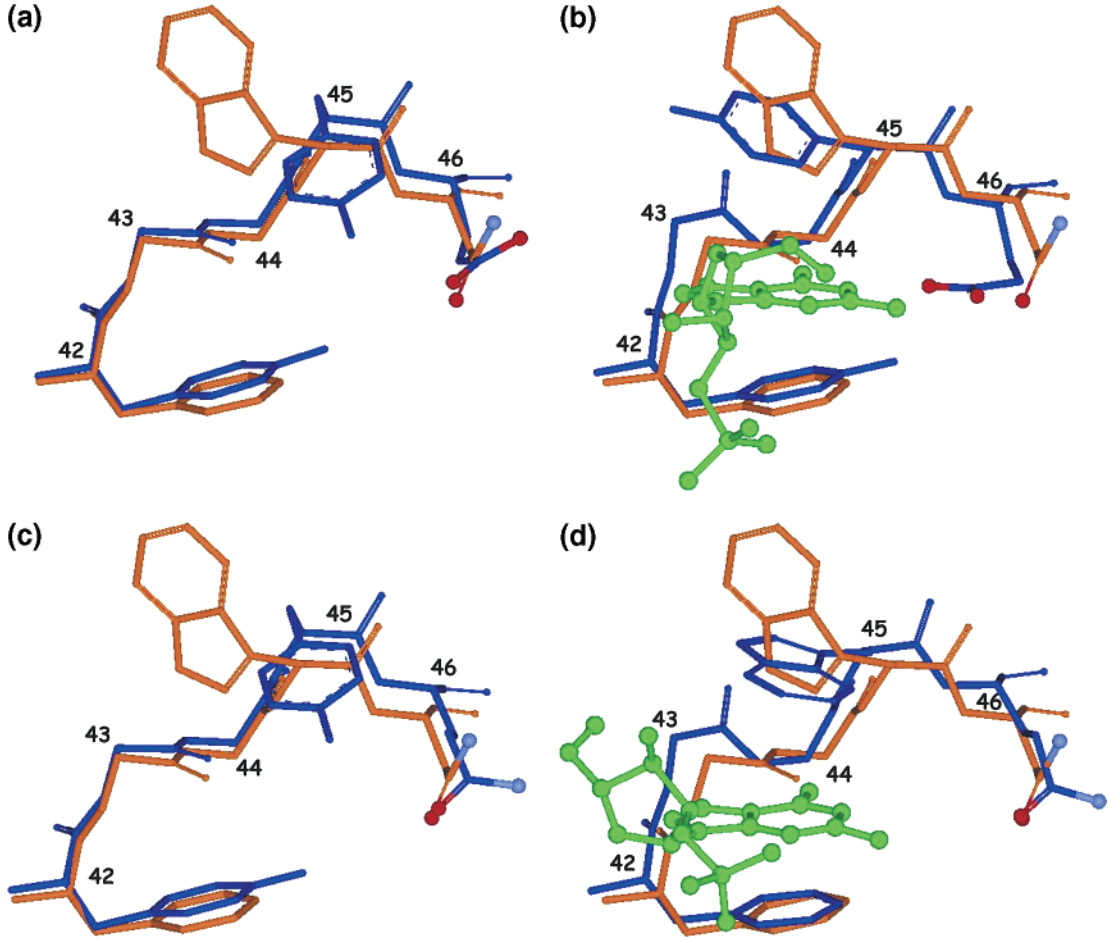

FIGURE 3: Comparison of the primary recognition sites of RNase T1 RV variants (orange) with previously determined structures (blue): (a) unoccupied RNase T1-wt, (b) RNase T1-wt complexed with 2′-GMP (note the change in the Tyr45 side chain relative to the unoccupied enzyme in panel a), (c) variant E46Q complexed with 2′-GMP (nucleotide not shown), and (d) variant 9/5 in complex with 2′-GMP. Amino acid side chains are drawn as sticks and bound 2′-GMP molecules as balls and sticks. The oxygen and nitrogen atoms of amino acid 46 are in red and light blue, respectively.

superposition of these three molecules shown in Figure 2 reveals, above all, significant differences within the nucleotide recognition loop (residues 41−46), indicating different sets of conformations, as the electron density for this region is well-defined in all three molecules. The abnormal disorder of the side chain of Val78 that was described for RNase T1-wt with an unoccupied primary recognition site (*10*, *12*) was not observed for variant RV.

Geometry of the Primary Recognition and Catalytic Site

Primary Recognition Site. The primary nucleotide recognition site of RNase T1 RV adopts a conformation similar to that found in other unoccupied recognition sites in RNase T1 (*10*−*13*). The crucial amino acid Glu46 in RNase T1-wt undergoes an induced fit during nucleotide binding. In the enzyme with an unoccupied recognition site, Glu46 is pulled out of this site to form hydrogen bonds with Asn99 and Phe100 (Figures 3a and 4a). In the presence of 2′-GMP in the primary recognition site, Glu46 is hydrogen-bonded to the guanine base (Figures 1a, 3b, and 4b). In the nearly inactive variant Glu46Gln (Figures 3c and 4c) and also in active variant 9/5 (Figures 3d and 4d), the glutamine in position 46 is held in the same conformation as in the uncomplexed wt enzyme. This is probably the result of a tight bidentate hydrogen bonding interaction between Gln46 and the backbone of Phe100, even though 2′-GMP is bound to the active site of the enzyme in the case of variant 9/5. In variant RV, Asn46 seems to be more flexible than Gln46 in variants Glu46Gln and 9/5. The hydrogen bond network and also the conformation of Asn46 differ slightly between the three RNase T1 RV molecules in the asymmetric unit (see Table 2).

Crystal structure analyses of RNase T1 with unoccupied recognition sites revealed an altered orientation of the peptide bond between asparagines 43 and 44 that flips due to the induced fit if guanine enters the binding site. However, in the structure of RNase T1 RV, both characteristic conformations are realized. In molecule C, this peptide bond adopts a conformation comparable to that of the wild-type enzyme with an unoccupied recognition site, whereas in molecule B, this bond rotates by ∼110°, resembling a conformation that is found in the wild-type with bound 2′-GMP. In molecule A, both possibilities are found as alternative conformations (see the electron density map of this area in molecule A in Figure 5). The primary recognition site of RNase T1 RV is filled with three water molecules that fill the nucleotide binding site and are found in similar positions in RNase T1-wt with an unoccupied recognition site (*11*) as well as in the wt 2′-AMP complex where the nucleotide is bound to the 3′-subsite and stacks on His92 (*10*).

In the wt 2′-GMP complex, the side chains of Tyr42 and Tyr45 are positioned such that they could form hydrophobic

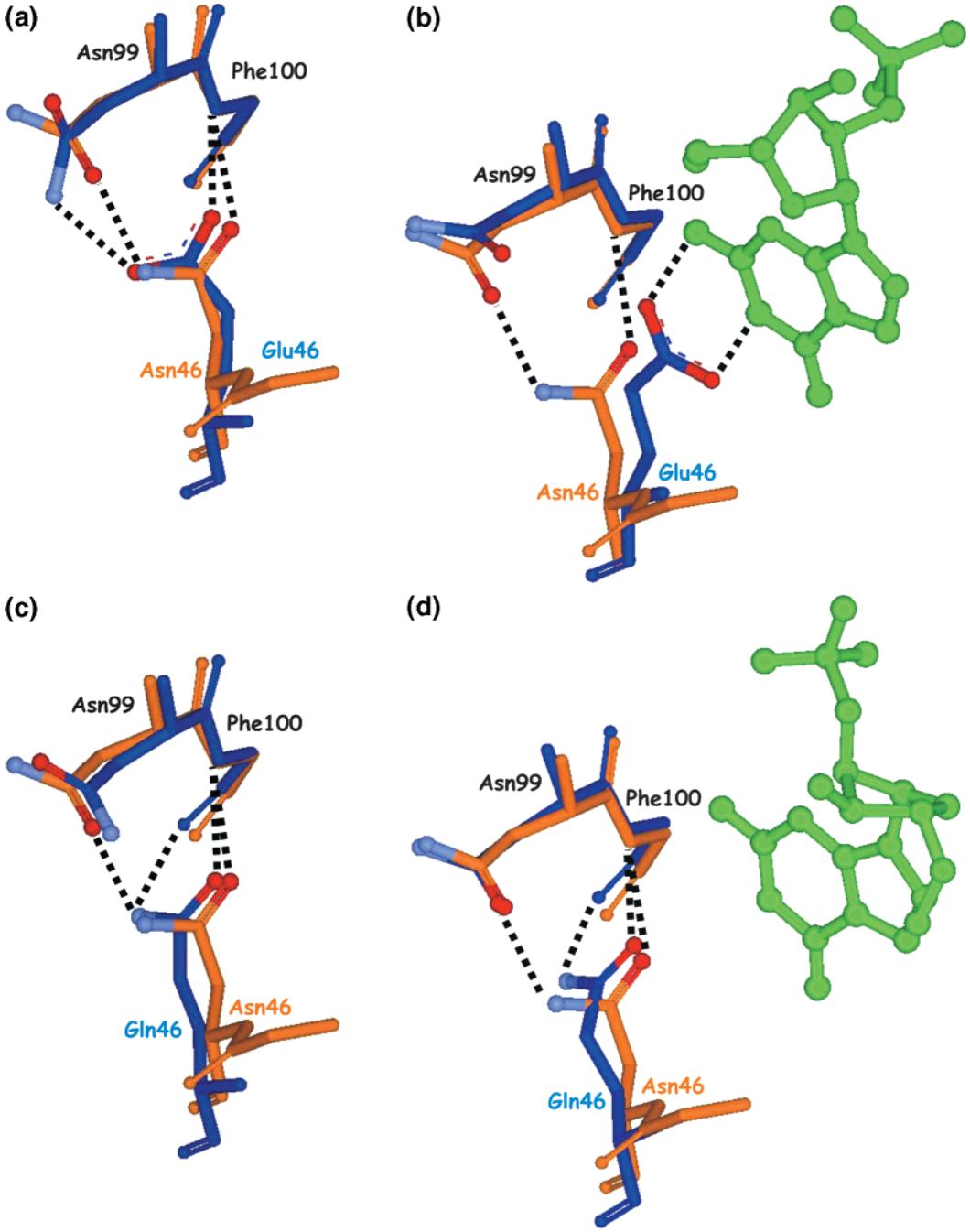

FIGURE 4: Comparison of the interactions of amino acid side chain 46 of RNase T1 RV (orange) with previously determined structures (blue): (a) unoccupied RNase T1-wt, (b) RNase T1-wt complexed with 2′-GMP, (c) variant E46Q complexed with 2′-GMP (nucleotide not shown), and (d) variant 9/5 in complex with 2′-GMP. Amino acid side chains are drawn as sticks and bound 2′-GMP molecules as balls and sticks. The oxygen and nitrogen atoms of amino acid 46 are in red and light blue, respectively.

stacking interactions with the guanine. It is supposed that the side chain of Tyr45 acts as a lid that covers the nucleobase (*11*, *17*). Because of the conformation of Glu46 in unoccupied RNase T1-wt, Tyr45 is pulled toward this recognition site (Figure 3a,b). In the nearly inactive variant Glu46Gln, this conformation is locked because of the bidentate hydrogen bond of Gln46, and consequently, the binding of the guanine and also adenine is not possible. In variant RV, the tryptophan at position 45 shows a high flexibility as shown by the different conformations within molecules A−C and by the slight disorder indicated by the electron density of Trp45 in molecules B and C. However, Phe42 as part of the protein core exhibits a rigid conformation. The similar positions of Phe42 in the three molecules in the T1 RV crystals and of the corresponding Tyr42 in the wt enzyme indicate the importance of the phenyl ring system and its conformational rigidity for RNase T1 activity. The Tyr42Trp substitution led to a variant with a strongly decreased turnover number for GpC cleavage (*14*).

Catalytic Site. The catalytic site of RNase T1 is formed by Tyr38, His40, Glu58, Arg77, and His92, which bind the phosphate moiety of the nucleotide. In RNase T1 RV at this position, a Tris molecule is bound in molecules A and C (see Figure 6). There is a good superposition of the Tris molecule in variant RV onto the phosphate moiety of 2′-GMP and 3′-GMP in the wt enzyme. All oxygens and the nitrogen of the Tris molecule are engaged in hydrogen bonding (see Table 3). The amino acid side chains of the

Table 2: Possible Hydrogen Bonding Interactions of Asn46 of the Three Molecules

atom of Asn46	hydrogen bonding partner	distance (Å)
	Molecule A	
N (main chain)	water91	2.86
Oδ1	F100 N	2.86
	water91	2.85
Nδ2	N99 Oδ1	2.92
	N98 Oδ1	3.14
O (main chain)	N99 Nδ2	2.98
	Molecule B	
N (main chain)	water93	2.98
Oδ1	F100 N	3.01
	water93	2.66
Nδ2	N99 Oδ1	3.28
O (main chain)	N99 Nδ2	2.98
	Molecule C	
N (main chain)	water57	2.73
Nδ2	water43	3.54
	N66 Oδ1	3.24

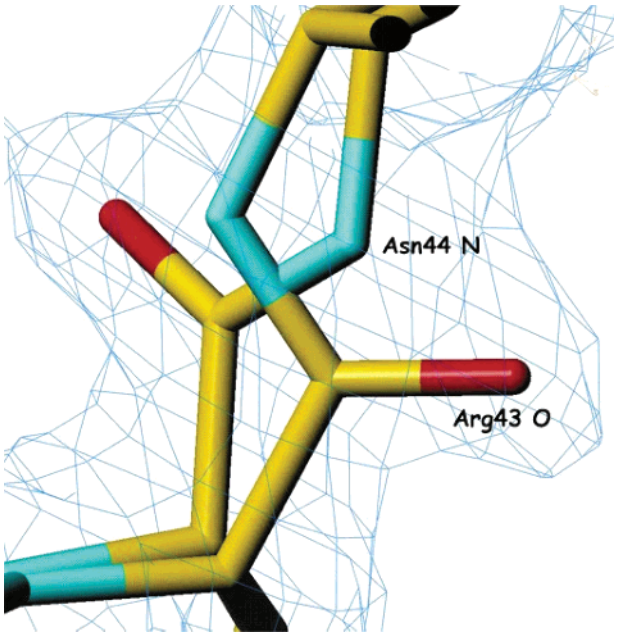

FIGURE 5: Electron density map ($2F_o - F_c$) around the Arg43−Asn44 peptide bond showing the alternative conformations of this peptide bond in molecule A. Nitrogen atoms are in cyan, oxygen atoms in red, and carbon atoms in yellow.

catalytic site are not only involved in binding Tris but also engaged in intramolecular hydrogen bonds with His40, His92, and Arg77 stabilized by side chain−main chain interactions and a salt bridge between Arg77 and Glu58 (see Table 3). Similar interactions are also found in uncomplexed RNase T1-wt (*12*) as well as in the vanadate (*11*) and 2′-AMP complexes (*10*), whereas binding of the Tris molecules is similar to the binding of the vanadate ion and the phosphate moiety of 2′-AMP. In the catalytic site of molecule B that has no bound Tris, these interactions are formed with water molecules occupying the corresponding binding sites (see Table 3). The conformations of His40 and His92 involved in catalysis are nearly the same in all variants. However, their imidazole rings are flipped with respect to the RNase T1-wt−2′-GMP complex (*6*), whereas conformations comparable to those in variant RV are found in the unoccupied RNase T1-wt (*12*).

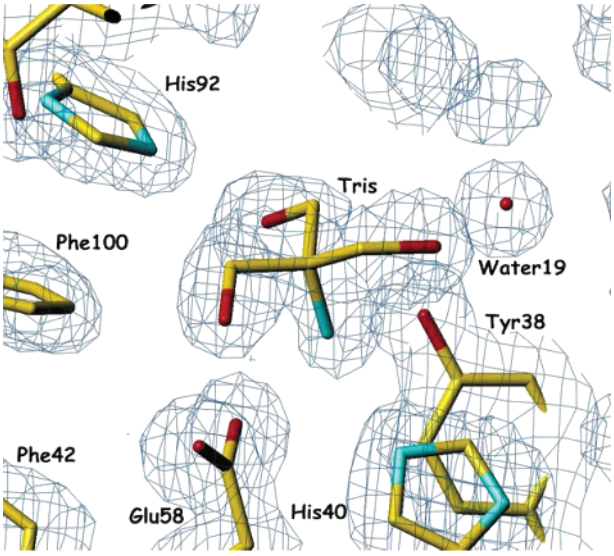

FIGURE 6: Electron density map ($2F_o - F_c$) of the catalytic site of molecule A with the bound Tris molecule. Nitrogen atoms are in cyan, oxygen atoms in red, and carbon atoms in yellow.

Table 3: Possible Hydrogen Bonding Interactions (distances in angstroms) between Catalytic Site Residues within the Three Molecules

	molecule A		molecule B		molecule C	
Y38 Oη	water19	2.61	water122	3.33	Tris O2	3.15
	Tris N	2.83	water209	2.65	Tris N	2.90
	R77 Nη2	3.17	R77 Nη2	3.25	R77 Nη2	3.16
H40 Nδ	N36 O	3.03	N36 O	2.91	E41 O	3.06
	S37 O	3.14	S37 O	2.86		
H40 Nϵ	Tris N	3.05				
E58 Oϵ1	Tris N	2.66	water122	3.75	Tris O3	3.04
	R77 Nϵ	3.03	R77 Nϵ	3.12	water64	2.87
E58 Oϵ2	Tris O3	2.70	water95	2.64	Tris O2	2.78
	water185	3.75	water108	3.19	R77 Nϵ	2.71
R77 Nη1	D76 O	2.79	D76 O	2.71	D76 O	2.83
	G74 O	2.89	G74 O	3.11	G74 O	2.88
R77 Nη2	Tris O2	2.73	N83 Oδ1	2.92	Tris O2	2.81
	G74 O	3.07	G74 O	3.16	G74 O	3.14
	Y38 Oη	3.17	Y38 Oη	3.25	Y38 Oη	3.16
H92 Nδ	N99 O	2.88	N99 O	2.96	N99 O	2.98
H92 Nϵ	Tris O2	2.57	water122	3.18	Tris O2	3.02

Cation Binding and Water Molecules. In RNase T1 RV, we found 274 water molecules that are hydrogen bonded to the three protein backbones, the side chains, and Tris molecules. The unoccupied primary recognition sites and the unoccupied catalytic site in molecule B are filled with water molecules that were also described for corresponding crystal structures. A comparison of RNase T1 structures in complex with 2′-GMP, 2′,5′-GpG, and vanadate indicated that there are structurally conserved water molecules (*37*). The reported hydrogen-bonded chain of 10 water molecules is also found partly in RNase T1 RV. In the wt enzyme, this chain can be divided into two parts, of which the first five water sites are also found in variant RV. This part of the water chain is thought to act as a space filler between the α-helix and the hairpin-like structure of the segment of residues 60−68. In RNase T1-wt, the water molecules of the second part are arranged around a Ca^{2+} ion coordinated to the Asp15 carboxylate. In RNase T1 RV, no cation is bound to the enzyme. Calcium ions were not added to the crystallization buffer as several crystallization experiments in the presence of calcium ions failed, in agreement with the finding that

Table 4: Kinetic Constants for Dinucleoside Phosphate Transesterification and RNA Hydrolysis of the RNase Wild-Type Enzyme and Variants RV, E46Q, and 9/5

enzyme	RNA hydrolysis[a] specific activity (units/mg)	GpC[a] K_m (μM)	GpC[a] k_{cat} (min^{-1})	GpC[a] k_{cat}/K_m (min^{-1} M^{-1})	ApC[a] K_m (μM)	ApC[a] k_{cat} (min^{-1})	ApC[a] k_{cat}/K_m (min^{-1} M^{-1})	specificity ratio $[k_{cat}/K_m(GpC)]/[k_{cat}/K_m(ApC)]$
wild-type[b]	384000[d] (100)	135 (100)	10200 (100)	750×10^5 (100)	–[f]	–[f]	264 (100)	284000
E46Q[c]	nd[e]	116 (85.9)	20 (0.2)	170.7×10^3 (0.23)	nd[e]	nd[e]	nd[e]	
9/5[d]	7091 (1.8)	979 (725.2)	444 (4.35)	453.5×10^3 (0.59)	nd[e]	nd[e]	nd[e]	
Glu46Ser/(insert)Gly[b]	nd[e]	–[f]	–[f]	222×10^3 (0.29)	–[f]	–[f]	2280 (863)	97
RV	5644 (1.5)	418 ± 28 (310)	327 ± 22 (3.2)	782.5×10^3 (1.04)	803 ± 63	16 ± 4	19925 (7547)	39

[a] Percent of wild-type values in parentheses. [b] From ref *39*. [c] From ref *13*. [d] From ref *21*. [e] Not determined. [f] Only k_{cat}/K_m could be determined.

the occupancy of these binding sites strongly depends on the crystal lattice (*38*). Indeed, Ca^{2+} is bound to Asp15 only in crystals of crystal form I, space group $P2_12_12_1$. In variant 9/5 that forms crystals that are not isomorphous to other variants, a Ca^{2+} is not bound to Asp15 but to the phosphate binding site of the enzyme.

Enzyme Kinetics

To determine the substrate specificity of variant RV, the hydrolysis of ApC and GpC was assessed and cleavage products were analyzed by thin-layer chromatography. The incubation of the enzyme with both dinucleoside phosphates for 15 min at room temperature yielded a significant hydrolysis of ApC as well as of GpC detected by the release of cytosine, whereas RNase T1-wt showed no detectable hydrolysis of ApC under the same conditions. To determine the steady state kinetic parameters, the dinucleoside phosphates were incubated with the enzyme for 10 min at 25 °C.

The kinetic constants determined for the dinucleoside phosphate cleavage from the spectrophotometric measurements as well as the RNA hydrolysis activities are summarized in Table 4, together with the corresponding kinetic parameters for RNase T1-wt and variants Glu46Gln, 9/5, and Glu46Ser/(insert)Gly (*13*, *21*, *39*).

The values of k_{cat} indicate that variant RV exhibits 3.2% GpC transesterification activity with respect to RNase T1-wt, whereas the value of k_{cat}/K_m decreases to 1% due to the increased value of K_m. If the RNA hydrolysis is compared, variant RV shows 1.5% of the wt activity. When compared to those of variant 9/5, the RNA hydrolysis and the value of k_{cat} differ only slightly. The substitution at position 46 therefore seems to have no effect on the velocity of the cleavage reaction, but the value of K_m for variant RV (Asn46) with GpC as the substrate is only approximately half of that for variant 9/5 (Gln46). This significant decrease in K_m indicates that Asn46 in variant RV participates in substrate recognition in contrast to Gln46 in variant 9/5 which was shown to be tightly hydrogen bonded to the backbone of Phe100 in the crystal structure of the variant 9/5−2′-GMP complex (*21*).

With variant RV, it was possible for the first time to determine single steady state kinetic parameters for a RNase T1 variant with ApC as the substrate. Kinetic analysis of ApC hydrolysis by variant RV results in an ~2-fold increased value of K_m compared to that of the hydrolysis of GpC. The k_{cat} of ApC cleavage is 16 min^{-1}, resulting in a k_{cat}/K_m value of $\sim 2 \times 10^4$ min^{-1} M^{-1} with ApC.

Another approach to changing the specificity of RNase T1 has been the enlargement of the binding site by the insertion of an additional random amino acid between positions 46 and 47 while position 46 was randomized as well. This led to variants with GpC/ApC specificity ratios of this library ranging from 2.84×10^5 for the wild-type to 97 for variant Glu46Ser/(insert)47Gly (*39*). Due to the very low enzymatic activity of this variant, individual kinetic parameters could not be determined. The decrease in the specificity constant (k_{cat}/K_m) for GpC cleavage to 222×10^3 M^{-1} min^{-1} (0.29% of the wt value) and the 8-fold increase in this constant for ApC cleavage result in this increased specificity ratio. The authors suggested that the reduction of the specificity ratio is more due to a decrease in the level of guanine recognition rather than to an increase in the level of adenine recognition. In variant RV, however, the increase in the activity for ApC is similar to the decrease in the activity for GpC. Compared to that of RNase T1-wt, the k_{cat}/K_m value for ApC cleavage was increased ~75-fold and the k_{cat}/K_m value for the GpC cleavage was reduced ~96-fold, resulting in a specificity ratio that was reduced 7250-fold.

CONCLUSIONS

Mutagenesis studies with RNase T1 performed so far show that there is no reliable way to predict amino acid substitutions leading to a desired altered specificity. Changing the substrate specificity of RNase T1 by a rational approach is difficult because the substrate recognition is mainly based on interactions with the peptide backbone. Both rational engineering and random mutagenesis did lead to a change in only the activity but not the specificity of the enzyme. In the work presented here, these two approaches were combined, and the RNase T1 RV was generated with a remarkable shift from guanine to purine specificity as shown by dinucleoside phosphate cleavage experiments. The values of K_m for the cleavage of dinucleoside phosphates ApC and GpC differ only by a factor of 2, whereas it is not possible to determine the value of K_m for the ApC cleavage of the wt enzyme or any RNase T1 variant known so far.

The starting point for this work was the well-characterized guanosine-specific RNase T1 variant 9/5 that arose from a random mutagenesis study (*20*, *21*) that differs from the wild-type in five amino acid positions within the guanine recognition loop. In this work, the specificity of this variant was changed by a further single-point mutation (Gln46Asn) within this recognition loop. Unfortunately, cocrystallization experiments with 2′-AMP and 2′-GMP have not been successful so far, but the crystal structure of the new variant without a bound nucleotide was determined and is in good

agreement with the kinetic and binding data (not shown). The primary recognition site resembles those that were found in all other structures of RNase T1 with an unoccupied primary recognition site. The tight hydrogen bonding of the amide group of glutamine in variants E46Q and 9/5 with the protein backbone of Phe100, however, was not observed with Asn46 variant RV (Figure 3c,d). Instead, the three molecules in the crystal asymmetric unit indicate a conformational flexibility of this region. The superposition of RNase T1 RV with variant 9/5 as well as with variant E46Q shows that the predicted loss of the ability to form the discussed H-bond due to the shortened amino acid side chain of Asn46 has not occurred and is compensated by a shift of the protein backbone. The conformations of Asn46 in variant RV and Gln46 in variants 9/5 and E46Q are nearly identical with respect to the amide group and the formation of the hydrogen bond between the backbone nitrogen of Phe100 and Gln Oϵ1 and Asn Oδ1, respectively. The second formed hydrogen bond, however, is different as Gln Nϵ2 is bound to the backbone oxygen of Phe100 in variants 9/5 and E46Q. By contrast in variant RV, Asn46 Nδ2 forms a hydrogen bond to Oδ1 of Asn99, comparable to the wt enzyme with an unoccupied recognition site except that the headgroup of Asn99 is rotated in the wild-type and therefore its Nδ2 is able to form a hydrogen bond to Glu46 Oϵ2. A superposition shows good agreement of Asn46 in variant RV and Glu46 in the wt with an unoccupied recognition site (Figure 4a). Comparison of the structures of the RNase T1−2′-GMP complex (*6*) and the uncomplexed enzyme (*11*, *12*) shows that in RNase T1-wt Glu46 changes its conformation when a nucleotide binds, and due to a similar conformation of Asn46, the same should hold for variant RV so that an interaction of Asn46 with guanine and with adenine should be possible, the latter causing the observed altered specificity. However, the mode of interaction of Asn46 with adenine and also with guanine needs to be determined.

Furthermore, the kinetic data also show the participation of Asn46 in the specific recognition of the nucleobase because of the halved value of K_m for GpC cleavage and a similar one for ApC cleavage compared to the K_m of variant 9/5 for GpC cleavage. Although the enzyme distinguishes in its binding only slightly between adenosine and guanosine, the cleavage rates of ApC and GpC differ considerably. Differences in the conformations of nucleotides adenosine and guanosine and therefore different positions of cleavable phosphodiester bonds are probably the reasons for this behavior because it is well-known that AMP prefers the anti whereas GMP prefers the syn conformation of the base relative to sugar (*40*). Moreover, the adenine is probably not saturated with hydrogen bonds, and due to the steric proximity of the peptidic N−H bond of both Arg43 and Asn44 and the N_6 amino group of adenosine (see Figure 1b), the base is presumably shifted somewhat or fully out of the binding pocket. A similar shift was also observed in variant 9/5 due to the narrowing of the guanine recognition site (*21*). An additional reason for such a shift of adenine is the possibility of the formation of a new hydrogen bond between adenine and the protein backbone. From RNase T1-wt, it is known that it undergoes an induced fit during binding of its substrate indicated by conformational changes of Tyr45 and Glu46 (see above) as well as a flip of the peptide group between Asn43 and Asn44 (*11*). This flip is energetically unfavorable as a left-handed helical conformation is introduced. If the flip would not occur when adenine binds, the formation of an additional hydrogen bond between N6 of adenine and N43-O is possible, resulting in a stabilization of adenine binding (Figure 7).

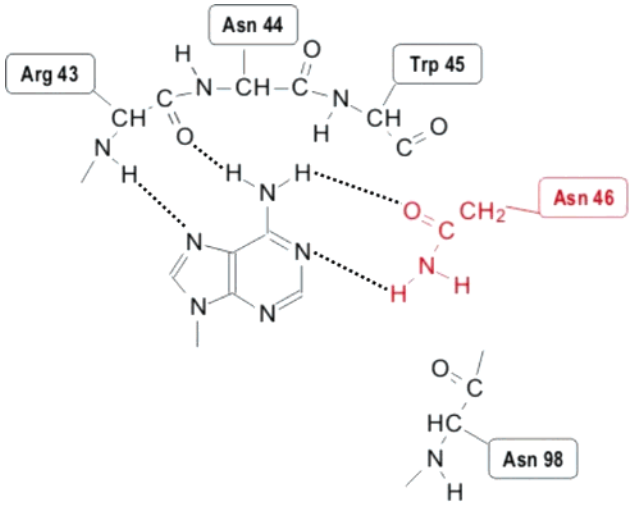

FIGURE 7: Sketch of the possible interaction of the adenine base with RNase T1 RV (note the additional possible hydrogen bond due to the flipped peptide bond between Arg43 and Asn44 in comparison to Figure 1b).

Variant RV exhibits the greatest reduction of the G/A specificity ratio observed for any variant to date and also is a purine-specific RNase T1 variant with the highest enzymatic activity. According to this, variant RV is the first variant of RNase T1 for which it was possible to determine single kinetic constants for the cleavage of not only GpC but also ApC; however, the mode of adenine recognition needs to be determined.

REFERENCES

1. Hill, C., Dodson, G., Heinemann, U., Saenger, W., Mitsui, Y., Nakamura, K., Borisov, S., Tishchenko, G., Polyakov, K., and Pavlovskii, S. (1983) The structural and sequence homology of a family of microbial ribonucleases, *Trends Biochem. Sci. 8*, 364−369.
2. Hartley, R. W. (1980) Homology between prokaryotic and eukaryotic ribonucleases, *J. Mol. Evol. 15*, 355−358.
3. Backmann, J., Doray, C. C., Grunert, H. P., Landt, O., and Hahn, U. (1994) Extended kinetic analysis of ribonuclease T1 variants leads to an improved scheme for the reaction mechanism, *Biochem. Biophys. Res. Commun. 199*, 213−219.
4. Heinemann, U., and Saenger, W. (1983) Crystallographic study of mechanism of ribonuclease T1-catalysed specific RNA hydrolysis, *J. Biomol. Struct. Dyn. 1*, 523−538.
5. Heinemann, U., and Saenger, W. (1982) Specific protein-nucleic acid recognition in ribonuclease T1−2′-guanylic acid complex: an X-ray study, *Nature 299*, 27−31.
6. Arni, R., Heinemann, U., Tokuoka, R., and Saenger, W. (1988) Three-dimensional structure of the ribonuclease T1 2′-GMP complex at 1.9-Å resolution, *J. Biol. Chem. 263*, 15358−15368.
7. Gohda, K., Oka, K., Tomita, K., and Hakoshima, T. (1994) Crystal structure of RNase T1 complexed with the product nucleotide 3′-GMP. Structural evidence for direct interaction of histidine 40 and glutamic acid 58 with the 2′-hydroxyl group of the ribose, *J. Biol. Chem. 269*, 17531−17536.
8. Heydenreich, A., Koellner, G., Choe, H. W., Cordes, F., Kisker, C., Schindelin, H., Adamiak, R., Hahn, U., and Saenger, W. (1993) The complex between ribonuclease T1 and 3′GMP suggests geometry of enzymic reaction path. An X-ray study, *Eur. J. Biochem. 218*, 1005−1012.
9. Koepke, J., Maslowska, M., Heinemann, U., and Saenger, W. (1989) Three-dimensional structure of ribonuclease T1 complexed

with guanylyl-2′,5′-guanosine at 1.8 Å resolution, *J. Mol. Biol. 206*, 475−488.
10. Ding, J., Koellner, G., Grunert, H. P., and Saenger, W. (1991) Crystal structure of ribonuclease T1 complexed with adenosine 2′-monophosphate at 1.8-Å resolution, *J. Biol. Chem. 266*, 15128−15134.
11. Kostrewa, D., Choe, H. W., Heinemann, U., and Saenger, W. (1989) Crystal structure of guanosine-free ribonuclease T1, complexed with vanadate (V), suggests conformational change upon substrate binding, *Biochemistry 28*, 7592−7600.
12. Martinez-Oyanedel, J., Choe, H. W., Heinemann, U., and Saenger, W. (1991) Ribonuclease T1 with free recognition and catalytic site: crystal structure analysis at 1.5 Å resolution, *J. Mol. Biol. 222*, 335−352.
13. Granzin, J., Puras-Lutzke, R., Landt, O., Grunert, H. P., Heinemann, U., Saenger, W., and Hahn, U. (1992) RNase T1 mutant Glu46Gln binds the inhibitors 2′GMP and 2′AMP at the 3′ subsite, *J. Mol. Biol. 225*, 533−542.
14. Grunert, H. P., Landt, O., Zirpel-Giesebrecht, M., Backmann, J., Heinemann, U., Saenger, W., and Hahn, U. (1993) Trp59 to Tyr substitution enhances the catalytic activity of RNase T1 and of the Tyr to Trp variants in positions 24, 42 and 45, *Protein Eng. 6*, 739−744.
15. Hakoshima, T., Tanaka, M., Itoh, T., Tomita, K. I., Amisaki, T., Nishikawa, S., Morioka, H., Uesugi, S., Ohtsuka, E., and Ikehara, M. (1991) Hydrophobic effects on protein/nucleic acid interaction: enhancement of substrate binding by mutating tyrosine 45 to tryptophan in ribonuclease T1, *Protein Eng. 4*, 793−799.
16. Loverix, S., Doumen, J., and Steyaert, J. (1997) Additivity of protein-guanine interactions in ribonuclease T1, *J. Biol. Chem. 272*, 9635−9639.
17. Nishikawa, S., Morioka, H., Kimura, T., Ueda, Y., Tanaka, T., Uesugi, S., Hakoshima, T., Tomita, K., Ohtsuka, E., and Ikehara, M. (1988) Increase in nucleolytic activity of ribonuclease T1 by substitution of tryptophan 45 for tyrosine 45, *Eur. J. Biochem. 173*, 389−394.
18. Steyaert, J., Opsomer, C., Wyns, L., and Stanssens, P. (1991) Quantitative analysis of the contribution of Glu46 and Asn98 to the guanosine specificity of ribonuclease T1, *Biochemistry 30*, 494−499.
19. Hirono, S., and Kollman, P. A. (1991) Relative binding free energy calculations of inhibitors to two mutants (Glu46→Ala/Gln) of ribonuclease T1 using molecular dynamics/free energy perturbation approaches, *Protein Eng. 4*, 233−243.
20. Hubner, B., Haensler, M., and Hahn, U. (1999) Modification of ribonuclease T1 specificity by random mutagenesis of the substrate binding segment, *Biochemistry 38*, 1371−1376.
21. Höschler, K., Hoier, H., Hubner, B., Saenger, W., Orth, P., and Hahn, U. (1999) Structural analysis of an RNase T1 variant with an altered guanine binding segment, *J. Mol. Biol. 294*, 1231−1238.
22. Landt, O., Grunert, H. P., and Hahn, U. (1990) A general method for rapid site-directed mutagenesis using the polymerase chain reaction, *Gene 96*, 125−128.
23. Quaas, R., McKeown, Y., Stanssens, P., Frank, R., Blocker, H., and Hahn, U. (1988) Expression of the chemically synthesized gene for ribonuclease T1 in *Escherichia coli* using a secretion cloning vector, *Eur. J. Biochem. 173*, 617−622.
24. Landt, O., Zirpel-Giesebrecht, M., Milde, A., and Hahn, U. (1992) Improving purification of recombinant ribonuclease T1, *J. Biotechnol. 24*, 189−194.
25. Zabinski, M., and Walz, F. G., Jr. (1976) Subsites and catalytic mechanism of ribonuclease T: kinetic studies using GpC and GpU as substrates, *Arch. Biochem. Biophys. 175*, 558−564.
26. Imazawa, M., Irie, M., and Ukita, T. (1968) Substrate specificity of ribonuclease from *Aspergillus saitoi*, *J. Biochem. 64*, 595−602.
27. Pace, C. N., Vajdos, F., Fee, L., Grimsley, G., and Gray, T. (1995) How to measure and predict the molar absorption coefficient of a protein, *Protein Sci. 4*, 2411−2423.
28. Anfinsen, C. B., Redfield, R. R., Choate, W. L., Page, J., and Carroll, W. R. (1964) Studies on the cross structure, cross-linkages and terminal sequences in ribonuclease, *J. Biol. Chem. 207*, 201−210.
29. McPherson, A. (1982) *The preparation and analysis of protein crystals*, John Wiley, New York.
30. Otwinowski, Z., and Minor, W. (1997) Processing of X-ray diffraction data collected in oscillation mode, *Methods Enzymol. 276*, 307−326.
31. Rossmann, M. G. (1972) *The molecular replacement method: A collection of papers on the noncrystallographic symmetry*, Gordon and Breach, New York.
32. Navaza, J. (1994) AMoRe: an automated package for molecular replacement, *Acta Crystallogr. A50*, 157−163.
33. Collaborative Computational Project (1994) The CCP4 Suite: programs for protein crystallography, *Acta Crystallogr. D50*, 760−763.
34. Brunger, A. T., Adams, P. D., Clore, G. M., DeLano, W. L., Gros, P., Grosse-Kunstleve, R. W., Jiang, J. S., Kuszewski, J., Nilges, M., Pannu, N. S., Read, R. J., Rice, L. M., Simonson, T., and Warren, G. L. (1998) Crystallography & NMR system: A new software suite for macromolecular structure determination, *Acta Crystallogr. D54*, 905−921.
35. Jones, T. A., Zou, J.-Y., Cowan, S. W., and Kjeldgaard, M. (1991) Improved methods for building protein models into electron density maps and the location of errors in these models, *Acta Crystallogr. A47*, 110−119.
36. Brunger, A. T. (1992) The free R-value: a novel statistical quantity for assessing the accuracy of crystal structures, *Nature 355*, 472−475.
37. Malin, R., Zielenkiewicz, P., and Saenger, W. (1991) Structurally conserved water molecules in ribonuclease T1, *J. Biol. Chem. 266*, 4848−4852.
38. Deswarte, J., De Vos, S., Langhorst, U., Steyaert, J., and Loris, R. (2001) The contribution of metal ions to the conformational stability of ribonuclease T1: crystal versus solution, *Eur. J. Biochem. 268*, 3993−4000.
39. Kumar, K., and Walz, F. G., Jr. (2001) Probing functional perfection in substructures of ribonuclease T1: double combinatorial random mutagenesis involving Asn43, Asn44, and Glu46 in the guanine binding loop, *Biochemistry 40*, 3748−3757.
40. Saenger, W. (1984) *Principles of Nucleic Acid Structures*, Springer-Verlag, Berlin.

BI035961F